Since January 2020 Elsevier has created a COVID-19 resource centre with free information in English and Mandarin on the novel coronavirus COVID-19. The COVID-19 resource centre is hosted on Elsevier Connect, the company's public news and information website.

Radiation Physics and Chemistry 179 (2021) 109168

Contents lists available at ScienceDirect

Radiation Physics and Chemistry

journal homepage: www.elsevier.com/locate/radphyschem

Gamma irradiation influence on mechanical, thermal and conductivity properties of hybrid carbon nanotubes/montmorillonite nanocomposites

Mou'ad A. Tarawneh[a,**], Sherin A. Saraireh[a], Ruey Shan Chen[b,*], Sahrim Hj Ahmad[b], Musab A.M. Al- Tarawni[c], Lih Jiun Yu[d]

[a] Department of Physics, College of Science, Al-Hussein Bin Talal University, P.O. Box 20, Ma'an, Jordan
[b] Department of Applied Physics, Faculty of Science and Technology, Universiti Kebangsaan Malaysia, 43600, UKM Bangi, Selangor Darul Ehsan, Malaysia
[c] Faculty of Engineering and Environment, Universiti Kebangsaan Malaysia, 43600, UKM Bangi, Selangor Daru Ehsan, Malaysia
[d] Faculty of Engineering, Technology and Built Environment, UCSI University, Kuala Lumpur Campus (North Wing), 56000, Cheras, Kuala Lumpur, Malaysia

ARTICLE INFO

Keywords:
CNTs
MMT
Thermomechanical
Electrical properties

ABSTRACT

A thermoplastic elastomer (TPE) based nanocomposite with the same weight ratio of hybrid nanofillers composed of carbon nanotubes (CNTs) and montmorillonite nanoclay (DK4) was prepared using a melt blending technique with an internal mixer. The TPE composite was blended from polylactic acid (PLA), liquid natural rubber (LNR) as a compatibilizer and natural rubber (NR) in a volume ratio of 70:10:20, respectively. The weight ratio of CNTs and DK4 was 2.5 wt%. The prepared samples were exposed to gamma radiation at range of 0–250 kGy. After exposure to gamma radiation, the mechanical, thermo-mechanical, thermal and electrical conductivity properties of the composites were significantly higher than unirradiated TPE composites as the irradiation doses increased up to 150 kGy. Transmission electron microscopy (TEM) micrographs revealed the good distribution and interaction between the nano-fillers and the matrix in the prepared TPE hybrid nanocomposites. In summary, the findings from this work definite that gamma irradiation might be a viable treatment to improve the properties of TPE nanocomposite for electronic packaging applications.

1. Introduction

Thermoplastic elastomers (TPEs) are a type of polymer materials with the elastic performance of rubber and the processing ability of thermoplastics. TPEs have become the most rapidly increasing segment in the polymer industry. This significantly growing area provides an important business opportunity for individuals who can capitalize on the capabilities of this class of materials (Miedzianowska et al., 2019). The requirements for TPEs in various areas of industrial activity drive researchers to apply new solutions to meet their expectations. One of the methods to develop the properties of conventional TPEs is the addition of nanofillers, such as carbon nanotubes (CNTs), graphene nanoplates (GNPs) and nanoclay to meet the demands of ever more discriminating customers (Song, 2018).

Generally, polymer nanocomposites are prepared by dispersing organic or inorganic nanoparticles into any thermoset or thermoplastic elastomers, resulting in a significant enhancement in the properties of polymers (Müller et al., 2017). Nowadays, intensive research has been focused on nanomaterials through the hybridization of two or more nanoparticles to create several hybridized nanostructures with new/enhanced properties and synergistic functionalities for attaining excellent performance in advanced applications. According to Datsyuk et al., the addition of polybenzimidazole nanofiber mats filled with several types of nanosized carbon materials such as CNTs, GNPs, graphite and carbon black (CB), into an epoxy resin enhances the mechanical and thermal properties (Datsyuk et al., 2020). Zdiri et al. have studied the effects of different nanofillers such as clay, CNTs, silica, CB, $CaCO_3$, zinc oxide and other materials on a recycled polypropylene (rPP) matrix. The rPP nanocomposites with a low content of nanoparticles possess enhanced mechanical properties, thermal stability and rheological behavior (Zdiri et al., 2018). Recently, multifunctional nanostructured hybrid polymer composite reinforced with different nanoparticles has taken place in the field of material science. Therefore, it is necessary to examine the reinforcing mechanism of hybrid filler in the polymeric matrix which could provide foundation for the modeling and design of new high performance composite materials. Thakur et al. examined the effects of the hybrid CNTs and nanoclay contents on the mechanical properties of an epoxy composite using a finite element

* Corresponding author.
** Corresponding author.
E-mail addresses: moaath20042002@yahoo.com (M.A. Tarawneh), chen@ukm.edu.my (R.S. Chen).

https://doi.org/10.1016/j.radphyschem.2020.109168
Received 9 May 2020; Received in revised form 25 August 2020; Accepted 26 August 2020
Available online 17 October 2020
0969-806X/

model by considering the variation of interphase properties and random distribution of CNTs and nanoclay. They found that the CNTs/nanoclay hybrid significantly alters the stiffening effect on a hybrid composite (Thakur et al., 2016). It has been reported that the use of non-conducting nanoclays could improve CNTs dispersion and help to create volume exclusion (which is the conductive nanoparticle available zone) inside polymer matrix and thereby causing a reduction in percolation threshold (Sanusi et al., 2020). Liu and Grunlan (2007) reported that based on their research finding, the good synergy between clay and single-walled CNTs in epoxy matrix in terms of simultaneously improved electrical and mechanical behaviors may make this composite better suited for a variety of sensing, shielding and packaging application. Therefore, the focus of the characterization for hybrid CNTs/clay composites prepared in this study was placed on electrical and thermal conductivities beside mechanical properties and thermal stability.

Gamma irradiation is a very suitable technique for modifying the chemical and physical properties of nanocomposite materials (Mohamed et al., 2020; Paula et al., 2019; Rahman et al., 2019). Furthermore, researchers have focused on the gamma sterilization of polymers used in some technological areas, such as the cable, food packaging (Genovese et al., 2016) and biomedical industries to guarantee microbiological safeness (Farkas, 1998), particularly during the current coronavirus disease (COVID-19) pandemic. The properties of nanocomposites exposed to ionizing radiation have generally been determined using three simultaneously applied methods: (1) crosslinking of polymer chains through chain transfer reactions besides the recombination of polymer radicals (2) degradation of the matrix polymer chains via the action of primarily formed radicals, and (3) the radiation-induced damage of the reinforcing filler (Chmielewski et al., 2005).

Once a nanocomposite material is irradiated, energy deposits in a specifically localized area also might cause ionization, excitation and the breakage of chemical bonds with the creation of various free radical species. These free radicals might react more with the surrounding elements, causing the development of degradation and crosslinking products that potentially alter the properties of the materials. The degradation of polymer is considered as a macromolecular reaction mediated by the formation of small mass fragments, chain splitting, and production of free radicals, while the crosslinking of the polymer occurs by main chain free radicals reaction includes the creation of three dimensional structures, causing significant modifications in the properties of the materials (Makuuchi and Cheng, 2012; Negrin et al., 2018). Consequently, studies of the physical and chemical effects induced by radiation energy absorption by the polymer are necessary.

Previous studies have examined PLA and NR irradiated with gamma rays. In the study by Razavi et al. (2014), PLA suffers strong oxidative degradation upon gamma irradiation. A 10% reduction in the glass transition is observed when PLA is irradiated with 50 kGy, indicating the dominance of the chain scission of PLA molecules during irradiation with gamma rays. According to Zaidi et al. (2013), the neat PLA was substantially degraded by gamma irradiation, while PLA-clay nanocomposites were less affected, as this treatment promotes the distribution of clay layer within the PLA matrix. On the other hand, NR is categorized as a radiation crosslinking type of polymer as it contains a double bond in the basic cis 1,4 polyisoprene unit. NR shows a linear increase in the tensile modulus as the irradiation dose increases from 0 to 250 kGy, primarily due to an increase in the crosslinking density as verified by Moustafa et al. (2016).

Although several reports have described the effect of gamma radiation on the properties and structures of polymer materials or single fiber composites (Kumar et al., 2020; Mammadov et al., 2017; Romanov et al., 2018), this study appears to be a new approach that concentrates on the effect of gamma radiation on the hybridization of CNTs/nanoclay based on TPE matrix nanocomposites. The aim of the current study was to examine the effect of various gamma irradiation doses on TPE nanocomposites containing 2.5 wt% carbon nanotubes and 2.5 wt% montmorillonite. The evolution of TPE nanocomposites in terms of the mechanical behavior, thermal properties, electrical conductivity and morphologies was investigated and the mechanism underlying the effect of gamma radiation was presented.

2. Experimental section

2.1. Materials

Polylactic acid (PLA) with a grade of 3251D was provided by Unic Technology Ltd., China. It has a density of 1.24 g cm^{-3} and a melt flow index of 30–40 g/10 min (190 °C/2.16 kg). SMR-L grade natural rubber (NR) was supplied by Guthrie (M: Manufacturer) Sdn. Bhd., which has a density 0.915 g cm^{-3}. Liquid natural rubber (LNR) was self-synthesized from NR using the photosensitized chemical oxidation technique in our research laboratory (Zailan et al., 2019). The LNR has the same microstructure with NR but with short chain of polyisoprene (different in molecular weight, Mw) at around 50 000 in comparison to NR with Mw of 900 000. It has the functional groups such as –OH and –COOH that resulted from the modification of NR (Tarawneh et al., 2020), which is expected to induce interaction between the rubber and plastic interphase and thereby increasing the homogeneity of the blend. Multi-walled carbon nanotubes (CNTs) produced via catalytic chemical vapor deposition with a purity of > 95%, diameter > 8 nm and length of 10–30 μm were provided by Arkema (GraphistrengthTM C100). Montmorillonite, namely, NanolinDK-4 (DK4), was supplied by Zhejiang Feng Hong Clay Chemical Co., Ltd. NanolinDK-4 is a white powder with 70 wt% intercalation with alkyl amine (30 wt%) and presents a cation-exchange capacity of 115–120 meq/100g. DK4 was dried under a vacuum at 70 °C for 24 h before use.

2.2. Sample preparation

The indirect method was used to prepare the nanocomposites and included the mixing of CNTs and DK4 with LNR supported by an ultrasonic bath (70 W, 42 kHz) for 3 h, before it was melt blended with PLA and NR inside the internal mixer. The TPE composite in the present study had a PLA:LNR:NR composition of 70:20:10 (Yu et al., 2019) with the total CNTs-DK4 contents of 5.0 wt% (each 2.5 wt%). During the processing of this nanocomposite, rotor screw rotation of 110 rpm, temperature of 180 °C, and mixing time of 14 min were identified as be the best parameter set. The mixing of the blends began by first inserting the NR into the mixer, followed by the premixture of CNTs-DK4–LNR after 4 min, and then the PLA was introduced at 7 min. The whole mixing process took 14 min. The granules obtained at the end of the production process were pressed to thicknesses of 1 mm and 3 mm (in the mold of 15 cm wide and 15 cm length) using a hot and cold pressing machine (LP50, LABTECH Engineering Company LTD) at 190 °C and a pressure of 1000 lbf/in^2.

2.3. Gamma irradiation test

Samples were placed in ^{60}Co gamma cell type Excel 220. The energy of Co-60 gamma is 1.17 and 1.33 MeV, average 1.25 MeV. The samples were irradiated with different doses (100, 150, 200 and 250 kGy) in air at dose rate of 2.8 kGy/h at room temperature. Five types of TPE with different gamma radiation doses were coded and presented in Table 1.

2.4. Characterization

2.4.1. Mechanical testing

The tensile properties of samples were determined using a Testometric universal testing machine (TUTM model-M350-10CT) in accordance with the ASTM 412 standard procedure with a crosshead speed of 50 mm/min and a load cell of 5 kN. The sample dimension was 30 × 4 × 1 mm^3. The Izod impact test was conducted at velocity of

Table 1
TPE with various wt-% of nanofiller loading.

Sample ID	wt% CNTs	wt-% DK4	Dose (kGy)
TPE	0	0	0
Nanocomposites (NC0)	2.5	2.5	0
Nanocomposites (NC100)	2.5	2.5	100
Nanocomposites (NC150)	2.5	2.5	150
Nanocomposites (NC200)	2.5	2.5	200
Nanocomposites (NC250)	2.5	2.5	250

3.45 m/s and a load weight of 0.898 kg using the Ray-Ran Pendulum Impact System (RRPIS) in accordance with ASTM D 256-90b. The sample dimension was 63 × 12 × 3 mm^3. The average value from seven samples was reported for each composition.

2.4.2. Dynamic mechanical analysis

The dynamic mechanical thermal analyzer (DMTA model TA-2980) (TA Instruments), was used in the three-point bending mode. Amplitude of 30 μm and a frequency of 1 Hz were applied to test each sample. Measurements were recorded at heating rate of 5 °C/min, from −100 °C to 145 °C. The dimension of the samples was 76 × 1.3 × 3 mm^3.

2.4.3. Thermal conductivity

The laser flash method measures thermal diffusivity and this method has been applied to derive thermal conductivity. Measurements of specific heats and thermal conductivities of samples (one specimen was tested per composite type) were measured using a thermal conductivity analyzer (TCA Nanoflash NETZSCH- model LFA 44712-41). Disc-type samples (diameter of 12.7 mm and thickness of 1 mm) were placed in the electric furnace. The thermal conductivity (λ, W $m^{-1}K^{-1}$) of samples depends upon the thermal diffusivity (α, mm^2 s^{-1}) and density (ρ, g cm^{-3}), and the change in which caused by the introduction of a reinforcing filler is negligible since it was added in a very small quantity compared to the TPNR matrix with an average density of 0.91 g cm^{-3}, and specific heat capacity (Cp, J g^{-1} K^{-1}) were calculated at various temperatures ranging from 25 °C to 155 °C using the following equations:

$$\lambda(T) = \alpha(T).\ \rho(T).\ Cp(T) \tag{1}$$

$$\alpha = 0.1388\left(\frac{d^2}{t_{1/2}}\right) \tag{2}$$

$$Cp = \frac{Q}{\rho dA}\cdot\frac{1}{\Delta T_{max}} \tag{3}$$

where d is the thickness of the sample in mm, $t_{1/2}$ is the time to the half maximum (when T/T_{max} reaches 0.5), ρ is the density of the sample, Q is the energy absorbed by the sample, A is the surface area of the sample, and T_{max} is the maximum rear-side increase in temperature. For the heat capacity calculations, a 12.7-mm-thick reference specimen of pyroceram was used.

2.4.4. Electrical conductivity

The electrical conductivity of the samples was measured using a high frequency response analyzer (HFRA Solartron 1256; Schlumberger) in the frequency range of 0.1 Hz–1 MHz. The surface of the sample was coated with the silver paint to allow the specimen surface to be conductive and to avoid charging, and then the sample was placed between the disc metal shape of the sample holder with a surface contact area of 2 cm^2. The bulk resistance (R_b (Ω)) of the samples was determined using Z-View software from the cole–cole plots. The electrical conductivity (σ) was calculated using the equation:

$$\sigma = L/R_b\ A \tag{4}$$

where L is the thickness of the sample (cm) and A (cm^2) is the effective contact area of electrode and electrolyte.

2.4.5. Transmission electron microscopy

The morphology of TPE and TPE nanocomposites was studied using transmission electron microscopy (TEM) (Philips model STEM CM12) with an accelerating voltage of 100 kV. An ultrathin piece of sample was prepared using a Leica ultracut E microtome with a cryo FC4E attachment at −100 °C.

2.4.6. ANOVA

The measured data for the mechanical, thermal and electrical conductivity properties were statistically compared using one-way analysis of variance (ANOVA) with the aid of the Data Analysis ToolPak in Microsoft Excel to determine the significance level (5%) of the effect of the gamma radiation dose.

3. Results and discussion

3.1. Mechanical properties

The effects of the gamma radiation dose on the tensile properties and impact strength of TPE and TPE nanocomposites are described in Fig. 1. As shown in the figure, the incorporation of CNTs/DK4 into TPE increased the tensile strength and Young's Modulus in the samples with 0 kGy. Moreover, in the presence of equal amounts of filler, the greatest tensile strength and Young's modulus for nanocomposites were obtained at 150 kGy radiation absorbed dose, which increased by approximately 44% and 47%, respectively, compared with TPE whereas the values improved by approximately 12% and 16%, respectively, compared to NC0. Thus, a gamma radiation dose of 150 kGy was considered as the optimum dose to obtain higher tensile strength and Young's modulus values. This difference may be attributed to the improved dispersion of the nanofiller contents in which the interaction of gamma radiation with the polymer causes a crosslinking between the polymer chains (Abdel-Rahman et al., 2018; Al Naim et al., 2017; Tüzemen et al., 2017). The greater crosslinking density of TPE blends revealed the potential presence of extra C–C bonds in the system, which is beneficial for stress transfer from the matrix to the filler in the process of stretching (Al Naim et al., 2017; Ismail and Mustapha, 2018; Tüzemen et al., 2017). Furthermore, the absorption of gamma ray energy increases the kinetic energy of CNTs and montmorillonite particles that manifests in any localized redistribution of nanoparticles in the host polymer chain; as a result, the density of the swelled nanoclay and dispersion of CNTs together permit polymer chains to be dispersed among the nanoclay layers to create exfoliation instead of intercalation and chain entanglement with CNTs (Al Naim et al., 2017; Müller et al., 2017). At higher radiation absorbed dose of 150 kGy, tensile strength and modulus of nanocomposites decreased considerably. The decrease in the value indicates that main chain was degraded and the polymer may become fragmented because of the increase in the energy at the same time as the clustering of CNTs and montmorillonite in the composite, as highlighted in the TEM results which are accountable for the low tensile properties (Tarawneh et al., 2013; Youssef et al., 2017).

The effects of CNTs/DK4 incorporation and the absorbed dose on the elongation at break (Fig. 1) are obvious. After exposure to a 150 kGy dose, a 40% loss in elongation at break due to radiation was observed, while the loss was 49% after exposure to a dose of 250 kGy. The elongation at break of composites was expected to decrease because of the formation of the network structure between the polymer and the filler (5 wt%) and the degree of crosslinking increased as the radiation dose increased. This significant increase might account for the decrease in the elongation at break which make composites inflexible and harder (Menacher et al., 2017).

Based on the results of the impact strength test (Fig. 1), the increase in the radiation dose would be accompanied by an increasing impact

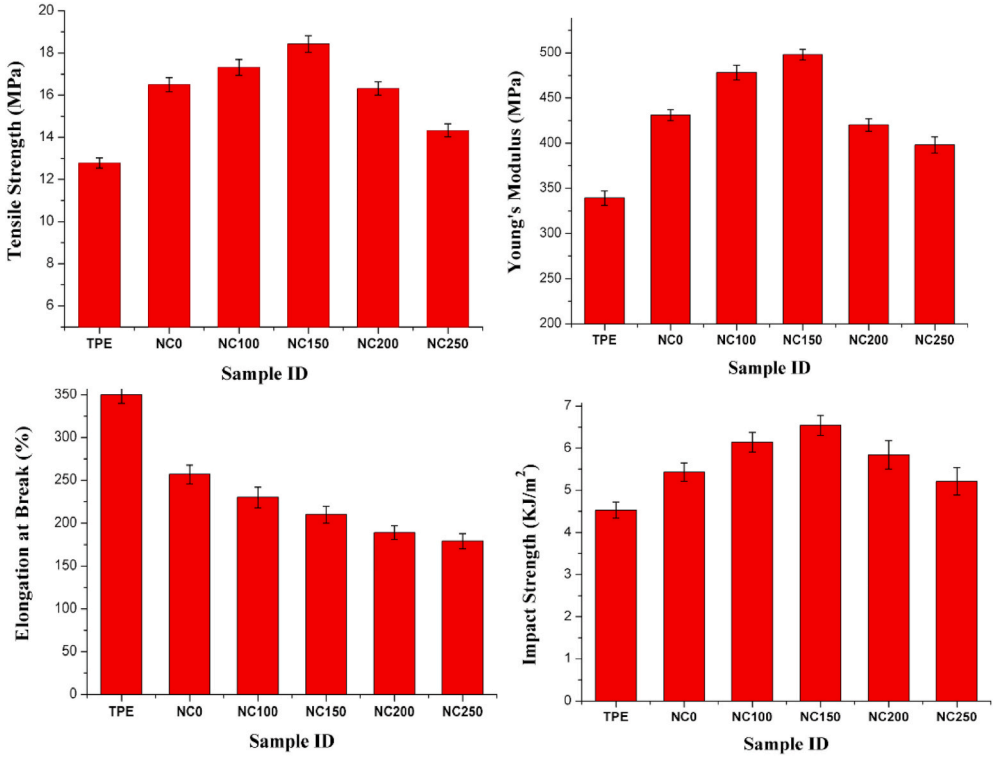

Fig. 1. The mechanical properties as a function of absorbed dose for TPE and TPE/CNTs/DK4 nanocomposites.

strength of the nanocomposite up to 150 kGy, followed by a decreasing trend as the dose increased up to 250 kGy. The impact strength of nanocomposites exposed to 150 kGy increased by approximately 44% and 21% compared with TPE and NC0, respectively. Following gamma radiation, the interfacial bond strength was increased by producing active sites (Li et al., 2015; Rui et al., 2015) inside the matrix and CNTs/DK4. Crosslinking and degradation occurred jointly upon radiation with the predominance of one to another, the ratio of crosslinking is higher than degradation at 150 kGy compared to higher radiation dose such as 250 kGy. Thus, an increase in the percentage of degradation is obvious in the absorbed dose range studied here. Nevertheless, the decrease in the impact strength at high radiation dose might be attributed to a degradation process including the scission of molecular chains of the blends and the rupture of chemical bonds, which in turn in the formation of internal micro-cracks (Chen et al., 2018; Rui et al., 2015). Furthermore, the agglomeration of nanoparticles inside the matrix might acts as defects and thus counteract any improvement due to the weak matrix-filler interaction.

According to the results of the statistical analyses (Table 2), the significance levels (*p*-values) for tensile strength, Young's modulus, elongation at break and impact strength were 4.80E-07, 5.05E-09, 6.58E-06 and 0.000228, respectively. These *p*-values are less than 0.05 and the *F* values are greater than the *F*-critical values for the same parameters. Therefore, those results confirmed the statistically significant differences in the effects of different gamma radiation doses.

Table 2
Repeated measures single-factor ANOVA of mechanical properties.

Properties	*F* value	*p*-value	*F* critical
Tensile Strength	62.747	4.80E-07	3.478
Young's Modulus	160.360	5.05E-09	3.478
Elongation at Break	35.969	6.58E-06	3.478
Impact Strength	16.197	0.000228	3.478

Note: *F* value, the mean between groups variance/mean within group variance; *p*-value, the probability of an *F* value ranging from 0 to 1; *F* critical, the critical *F* value based on the F distribution.

3.2. Thermo-mechanical properties

The influence of gamma irradiation dose on the storage modulus of TPE and TPE nanocomposites is presented in Fig. 2. For irradiated samples, the decreasing trend in the storage modulus with temperature was similar in NC0 and TPE due to the increase in chain movement at high temperatures. The effect of gamma irradiation on TPE nanocomposites was also visible from observations of the storage modulus value at −100 °C. A reasonable increase in the storage modulus value was achieved for the TPE nanocomposite at 150 kGy. This enhancement could be potentially attributed to the radiation induced crosslinking of polymer chains in the amorphous phase and the formation of rigid areas in the TPE matrix. Therefore, this crosslinked network caused the materials to become harder and inelastic, which provided more resistance to dynamic deformation. Nevertheless, beyond 150 kGy, the storage modulus value reduced back at the doses of 200 and 250 kGy. The reduction in the modulus is attributed to chain scission of the material (Ahmed et al., 2012; Colin et al., 2002) which contributed to the increase in the material brittleness (Ahmed et al., 2012; Perera et al., 2004).

The values of the glass transition temperature (T_g) were evaluated and plotted as a function of the gamma irradiation dose as shown in Fig. 3. The T_g increased with the gamma dose, and the highest value was recorded at a dose of 150 kGy. Therefore, the fillers in the TPE matrix might form a network of nano-particles that restricts the movement of the macromolecules; as a result, T_g of the matrix increased (Khare et al., 2015; Lafi and Imran, 2010). However, the T_g progressively reduced with an increasing dose up to 250 kGy dose as a result of chain scission which occurred readily inside the amorphous area. Furthermore, due to conglomerations, agglomerates existed in the matrix as a separated phase morphology among CNTs and montmorillonite, and these defects allow for free movement of the macromolecules; consequently, the T_g of nanocomposite was lower after exposure to high doses.

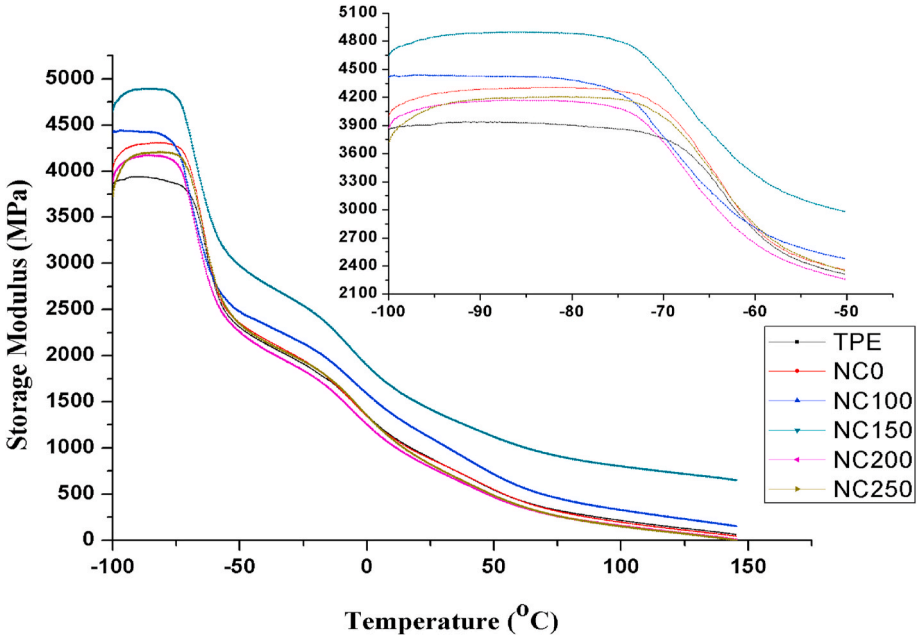

Fig. 2. Storage modulus for TPE and TPE/CNTs/DK4 nanocomposites with different absorbed doses as a function of temperature.

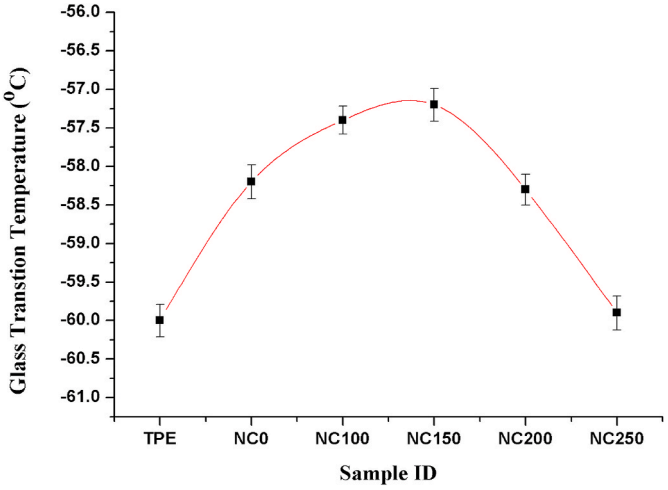

Fig. 3. Glass transition temperatures for TPE and TPE/CNTs/DK4 nanocomposites with different absorbed doses as a function of temperature.

Fig. 4 shows the dependence of the loss modulus of irradiated samples on the temperature. Mostly, the loss modulus curve of NC150 is displayed at higher values throughout the investigated temperature range as compared to other samples. This increase is ascribed to the more uniform distribution of CNTs/DK4 within the matrix of the NC150 samples. Thus, the interfacial area is larger and the interaction between the matrix and CNTs and montmorillonite is stronger due to the crosslinking increase. When the hybrid composites were subjected to external stress, the external energy was dissipated by the friction (Ahsan et al., 2016) between TPE/CNTs/CK4 interactions. As a result of the interaction between the polymer chains and the filler surface, the mobility of the macromolecular segments has decreased. This transition zone shows a higher modulus, which gradually decreases with the increasing distance from the filler surface at lower temperatures. As the temperature approached the region of the glass transition, the softening of the matrix and the initiation of the relaxation process started to occur through the activation of the molecular segmental motions. Nevertheless, this process involved a high level of dissipation of the force, thus increasing the loss modulus values. In the glass transition region, the chains were free to move, resulting in a rapid reduction in the loss modulus. This phenomenon is evidenced by the presence of sharp peak at approximately −70 to −50 °C.

3.3. Thermal conductivity

The thermal conductivity of the unirradiated and irradiated samples is shown in Fig. 5. Thermal conductivities of TPE and TPE nanocomposites increased with increasing temperature from 25 to 65 °C. Moreover, the effect of temperature on the thermal conductivity was negligible at temperatures greater than 65 °C. Remarkably, the conductivity of the nanocomposite at 150 kGy (NC150) was higher than the neat TPE or other nanocomposite at all measured temperatures as expected due to the crosslinking. The highly crosslinked samples (NC150) exhibited significant improvements in the thermal conductivity (from 25 °C to 145 °C) in contrast to nanocomposites treated with higher doses such as 200 kGy and 250 kGy because of the degradation is predominant along with the presence of agglomerated clusters inside

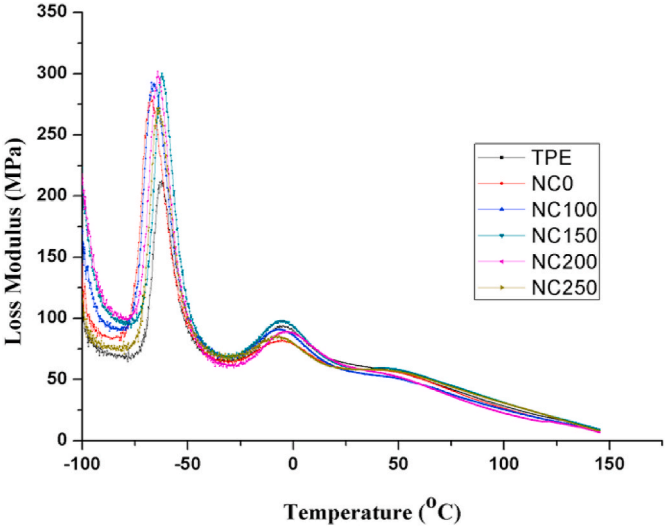

Fig. 4. Loss Modulus for TPE and TPE/CNTs/DK4 nanocomposites with different absorbed doses as a function of temperature.

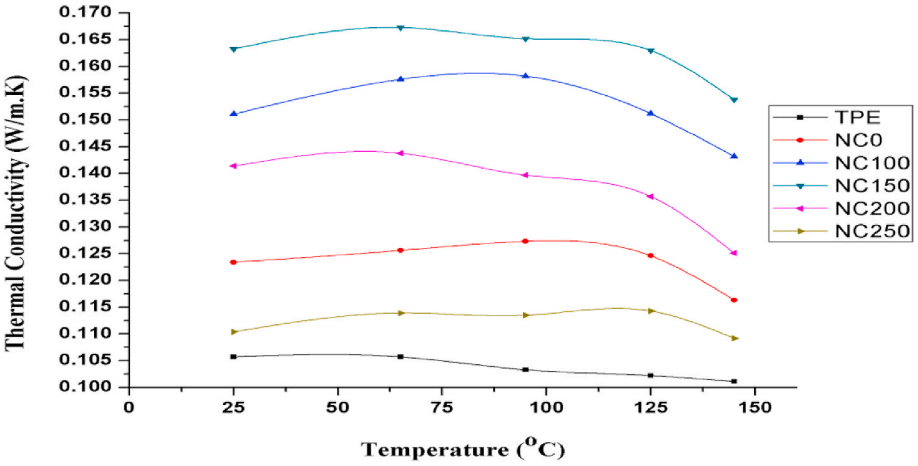

Fig. 5. Thermal conductivity of TPE and TPE/CNTs/DK4 nanocomposites with different absorbed doses as a function of temperature.

the matrix. This finding could be reconciled because there was a significant increase in the surface interface between CNTs/nanoclay filler and TPE matrix, which led to phonon scattering rate increase at the material interface in sample exposed to 150 kGy. In comparison, while the nanoparticles were agglomerated, the phonons choose to enter the particle phase, and therefore, the length of the polymer phase involved in phonon propagation became longer and the boundary resistance between the two phases acted a barrier for the heat flow and subsequently decreased the overall conductivity (Hida et al., 2013; Mehra et al., 2018). The appearance of agglomerated clusters is proposed to have caused the scattering of heat carrier phonons and decreased the flow of heat in a regular path; consequently, the thermal conductivity was reduced.

The effect of radiation on the thermal diffusivity of samples is presented in Fig. 6. As the temperature increased from 25 °C to 145 °C, a reduction in the thermal diffusivity was observed. This decrease is due to the opposing effects of temperature on the thermal diffusivity (Flaifel et al., 2013). Notably, the maximum thermal diffusivity was obtained for NC150 compared with other samples, which is similar to the results obtained for thermal conductivity. Besides the inherent characteristic of filler materials, the nanostructure and texture must be considered in which the thermal diffusivity of the composites is strongly dependent upon the thermal conductivity of the matrix and interconnectivity of the higher conducting phase due to the crosslinking at 150 kGy. As the test temperature increased, the phonon vibration frequency will be accelerated, and it will increase the opportunity of increasing the collisions. Consequently, the mean free path decreased quickly, and thus led to a rapid decrease in the thermal diffusivity. The reduced values of the phonon mean free path are attributed to the increasing number of defects and larger boundary at the interface of different phases of the nanocomposites (Flaifel et al., 2013; Gabr et al., 2015).

A two-factor analysis of variance without replication was used to examine the significance of the effects of the gamma irradiation dose and testing temperature on the thermal conductivity measurements of the nanocomposites. As shown in Table 3, the *p*-values for the thermal conductivity and diffusivity are less than the significance level (0.05), and the *F* values are larger than *F* critical for both investigated factors. These observations implied that both the irradiation doses and the varying test temperatures have significant contributions to the thermal conductivity properties.

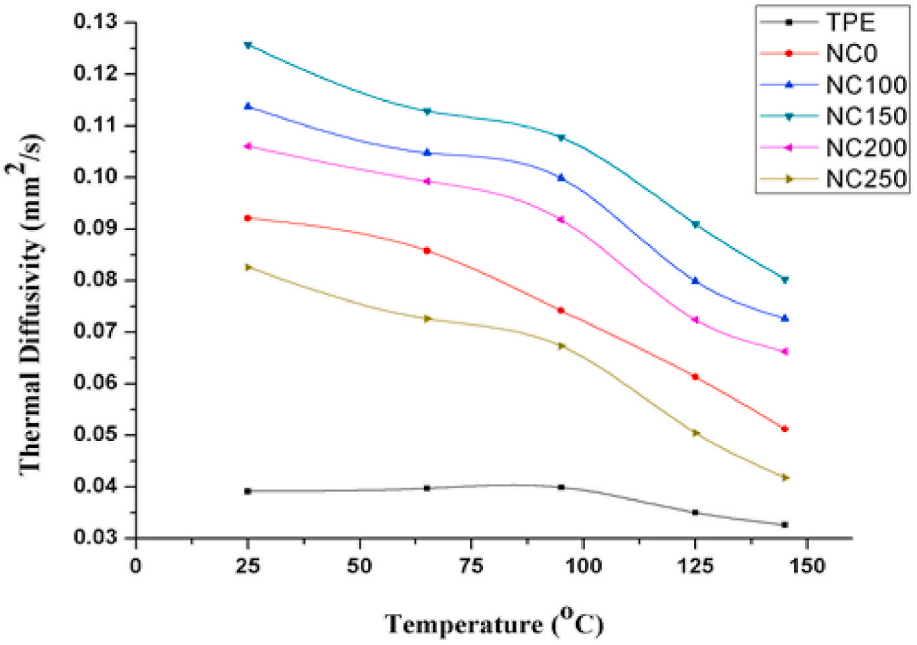

Fig. 6. Thermal diffusivity of TPE and TPE/CNTs/DK4 nanocomposites with different absorbed doses as a function of temperature.

Table 3
Two-factor ANOVA without replication of thermal conductivity and diffusivity.

Properties	*F* value (γ irradiation dose)	*F* value (temp)	*p*-value (γ irradiation dose)	*p*-value (temp)	*F* critical (γ irradiation dose)	*F* critical (temp)
Thermal conductivity	318.670	17.430	4.96E-15	1.11E-05	3.007	3.007
Thermal diffusivity	67.745	387.917	7.99E-10	1.05E-15	3.007	3.007

Notes: *F* value, the mean between groups variance/mean within group variance; *p*-value, the probability of an *F* value ranging from 0 to 1; *F* critical, the critical *F* value based on the F distribution.

Table 4
The electrical conductivity of TPE with different absorbed dose.

Sample ID	Dose (kGy)	Electrical Conductivity, σ (S/m)	Single Factor ANOVA
TPE	0	3.79×10^{-14}	*F* value: 1197.551
NC0	0	4.51×10^{-12}	*p*-value: 2.35E-13
NC100	100	2.38×10^{-10}	*F* critical: 3.478
NC150	150	1.41×10^{-9}	
NC200	200	4.14×10^{-11}	
NC250	250	8.62×10^{-12}	

3.4. Electrical conductivity

The electrical conductivity of the unirradiated and irradiated samples is shown in Table 4. Non irradiated TPE and TPE nanocomposite samples that were not treated with gamma irradiation exhibited electrical conductivities of 3.79×10^{-14} S/m and 4.51×10^{-12} S/m, respectively. Overall, the statistical analysis showed that the gamma irradiation treatment exerted a significant effect on the electrical conductivity properties of nanocomposites, as the *p*-value was less than 0.05 and the *F* value was less than *F* critical (Table 4). When the nanocomposites were exposed to gamma radiation at doses ranging from 100 kGy to 150 kGy, the electrical conductivity properties increased by approximately 4 and 2 orders of magnitude compared with TPE and NC0, respectively. Because of the separate phase between the CNTs and montmorillonite were effectively filled, and they were well-interacted as observed in TEM micrographs latter, resulting in the formation of conducting networks and the establishment of a proper percolating network structure in the matrix, the electrical conductivity increased. Furthermore, as expected, the NC250 and NC200 nanocomposites displayed poor performance in terms of electrical conductivity compared to NC150. The explanation for this observation is the poor contact of the CNTs and montmorillonite particles (as revealed by TEM results) caused by their randomly agglomerated shape and the low aspect ratio of unity that enabled them to form conducting networks in the TPE matrix at high doses (Paydayesh et al., 2019; Tarawneh et al., 2019). Furthermore, the degradation induced by the high-energy irradiation destroyed the crosslinked structure of the system (Ahmed et al., 2012; Perera et al., 2004), which decreased the electrical conductivity of the TPE/CNTs/DK4 nanocomposites.

3.5. Morphological analysis using TEM

The morphology of the samples was investigated by transmission electron microscopy (TEM). Fig. 7(A) and (B) show TEM micrographs of neat TPE and TPE/CNTs/DK4 before gamma irradiation (NC0), respectively. In Fig. 7(A), the morphology of neat TPE showed lighter areas attributed to the PLA phase while the darker areas as the rubber phase. However, in the absence of gamma irradiation (0 kGy), the morphology of the TPE/CNTs/DK4 nanocomposite exhibited irregularities of the dispersion of CNTs and montmorillonite as separated phases in the TPE matrix, as shown in Fig. 7(B). In Fig. 7(C) and (D) which corresponds to the TPE/CNTs/DK4 irradiated with radiation absorbed doses of 100 kGy and 150 kGy, respectively, the samples showed significant positive adhesion at interfaces between CNTs and montmorillonite. At an absorbed dose of 150 kGy, the TEM micrograph shows a better dispersion of CNTs and montmorillonite in TPE with a reduction in the size of the clay domain, as compared to other gamma radiation doses. Besides, the clay was dispersed in the state of intercalation or exfoliation in TPE matrix, as can be seen from the lighter grey colour of better separated clay layers in Fig. 7(D). Although the distribution between the nanoparticles of MMT and CNTs was still not perfectly uniform, it clearly indicated that gamma radiation promoted better interactions and improved the compatibility between the nanofiller and TPE. This improvement in the compatibility and entanglement between the components of the hybrid system was induced by the increase in the interfacial action due to the crosslinking that occurred upon exposure to an optimum dose of gamma ray (150 kGy). As shown in the TEM micrograph presented in Fig. 7(E) and (F), higher dose of gamma rays reduced the miscibility and the interfacial adhesion between CNTs, montmorillonite and TPE after the absorption of doses of 200 kGy and 250 kGy respectively. Based on the TEM results, it may be observed that by increasing the gamma dose to greater than 150 kGy, a morphological conversion happened where the size of the montmorillonite and CNTs agglomerates began to grow and exhibited a separated phase morphology between CNTs and montmorillonite with poor interactions at interfaces due to degradation. This phenomenon was similarly observed in the study of Zaidi et al. (2013), they reported that with increasing radiation to 100 kGy dose, a morphological change happened, where the orientation of silicate layers was destroyed, and the stacked clay layers were not randomly dispersed in PLA matrix. Therefore, the properties of the nanocomposites were adversely affected, as described above.

Fig. 8 shows a schematic model of the hybrid (CNTs/nanoclay) inside the TPE matrix exposed to the optimum gamma dose (150 kGy) and higher gamma dose. According to the TEM results, the performances of the nanocomposites strongly depend on the effect of the gamma radiation absorbed dose. After exposure to the optimum dose, the connections between the hybrid nanofiller components (CNTs/nanoclay) as a nano-unit and the TPE matrix form a linked network structure, resulting in the formation of a proper network structure in the matrix. The improved dispersion of the hybrid filler is obtained due to the crosslinked networks generated in non-crystalline areas of TPE which limit the congregation of these nanoparticles and keeping them randomly dispersed inside the matrix. However, upon irradiation especially after high absorbed gamma dose, it could alter the interactions of CNTs and nanoclay where the agglomeration of nanoparticles will be caused and existed in separated phase units inside the matrix. Moreover, the oxidation and scission of polymer chains are considerably intensified with the increasing gamma doses and thus forming molecular species with higher mobility (Lu et al., 2005) that encapsulate the separated units of CNTs and nanoclay. Therefore, a non-ordered structure is created when the irradiation dose increases, which is responsible for the decreased performances of the nanocomposites.

4. Conclusions

The results in the present study revealed the mechanical, thermal, conductivity and morphology properties of TPE composite and TPE nanocomposites prepared using melt processing. The effects of gamma radiation with different doses on modifying the properties of the nanocomposite were investigated. As displayed in the morphology

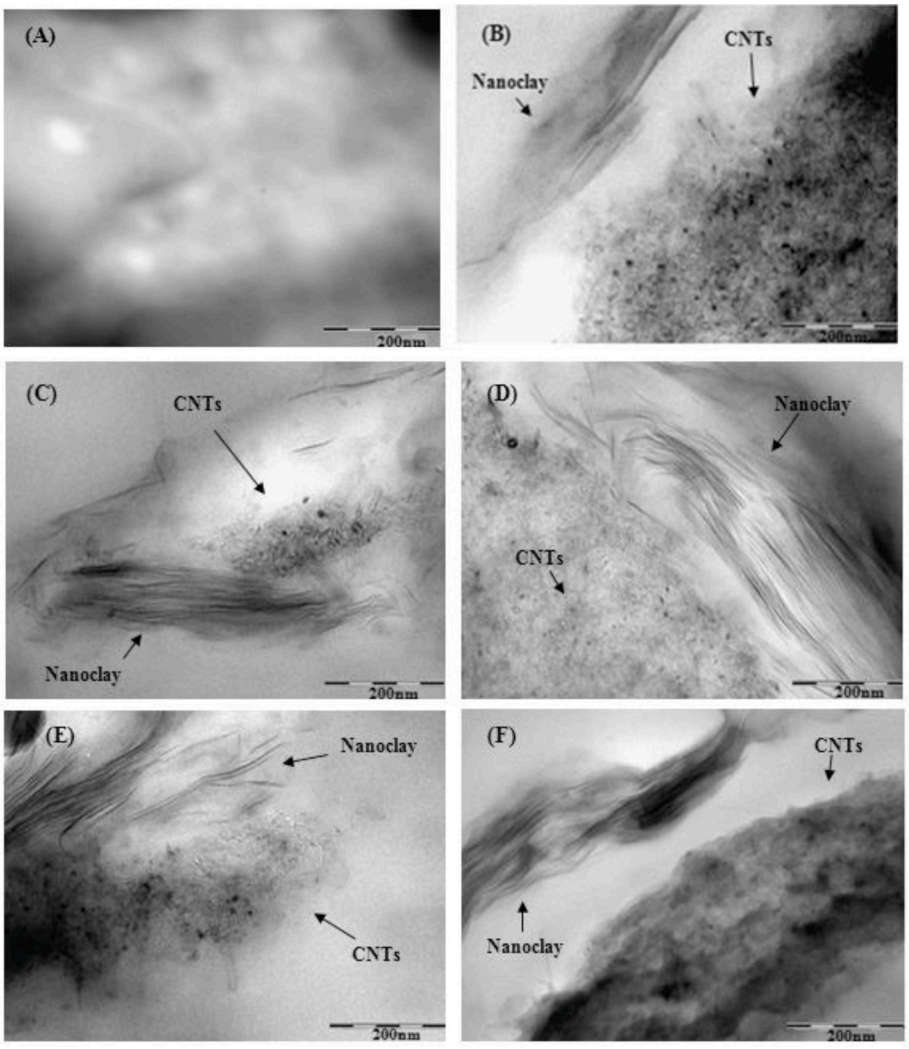

Fig. 7. TEM micrographs of (A) TPE, (B) NC0, (C) NC100, (D) NC150, (E) NC200, and (F) NC250.

observation, irradiation improved the interactions of CNTs/montmorillonite and promoted an improved nanofiller-dispersion in the matrix, resulting in an overall enhancement in the mechanical properties, thermo-mechanical properties, thermal conductivity and electrical conductivity properties, particularly in samples exposed to an optimal gamma radiation absorbed dose of 150 kGy. However, with further

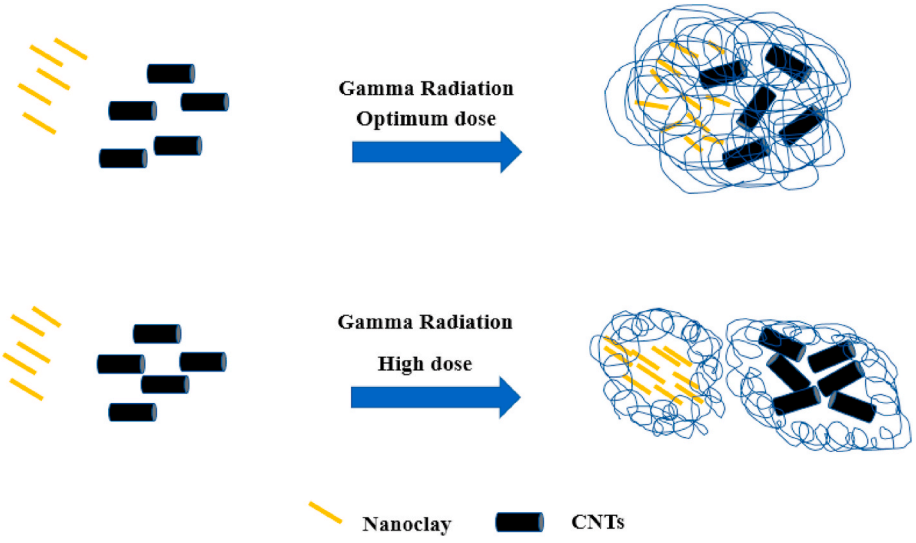

Fig. 8. A schematic model of the hybrid (CNTs-nanoclay) inside the TPE matrix after the exposure to the optimum gamma dose and high gamma dose.

increase of radiation dose greater than 150 kGy, the properties of the samples decreased. The radiation processing of TPE nanocomposites through exposure to a gamma radiation source is presented to illustrate the broad potential of this approach in industrial applications, such as electronic packaging, due to the excellent mechanical and conductive properties as exhibited by hybrid CNTs/montmorillonite nanocomposites gamma irradiated with 150 kGy radiation absorbed dose in this study.

CRediT authorship contribution statement

Mou'ad A. Tarawneh: Conceptualization, Methodology, Investigation, Data curation, Writing - original draft. **Sherin A. Saraireh:** Visualization. **Ruey Shan Chen:** Visualization, Formal analysis, Writing - review & editing. **Sahrim Hj Ahmad:** Supervision, Conceptualization, Funding acquisition. **Musab A.M. Al- Tarawni:** Investigation. **Lih Jiun Yu:** Visualization, Investigation.

Declaration of competing interest

The authors declare that they have no known competing financial interests or personal relationships that could have appeared to influence the work reported in this paper.

Acknowledgements

The authors would like to express their thanks to the Kementerian Pendidikan Malaysia (Grant ID: FRGS/1/2019/TK05/UKM/02/3) and Universiti Kebangsaan Malaysia for the financial support through the grants of DIP-2018-031, UKM-OUP-NBT-29-142/2011 and UKM-OUP-2012-135.

Appendix A. Supplementary data

Supplementary data related to this article can be found at https://doi.org/10.1016/j.radphyschem.2020.109168.

References

Abdel-Rahman, H., Younes, M., Yassene, A.A., 2018. Physico-mechanical properties of gamma-irradiated clay/polyester nanocomposites. Polym. Compos. 39, 3666–3675.
Ahmed, F.S., Shafy, M., El-Megeed, A.A., Hegazi, E.M., 2012. The effect of γ-irradiation on acrylonitrile–butadiene rubber NBR seal materials with different antioxidants. Mater. Des. 36, 823–828 1980-2015.
Ahsan, Q., Tee, Z.W., Rahmah, S., Chang, S.Y., Warikh, M., 2016. Wear and friction behaviour of magnesium hybrid composites containing silicon carbide and multi-walled carbon nanotubes. Adv. Mater. Process. Technol. 2, 303–317.
Al Naim, A., Alnaim, N., Ibrahim, S.S., Metwally, S., 2017. Effect of gamma irradiation on the mechanical properties of PVC/ZnO polymer nanocomposite. J. Rad. Res. Appl. Sci. 10, 165–171.
Chen, R.S., Ahmad, S., Gan, S., 2018. Rice husk bio-filler reinforced polymer blends of recycled HDPE/PET: three-dimensional stability under water immersion and mechanical performance. Polym. Compos. 39, 2695–2704.
Chmielewski, A.G., Haji-Saeid, M., Ahmed, S., 2005. Progress in radiation processing of polymers. Nucl. Instrum. Methods Phys. Res. Sect. B Beam Interact. Mater. Atoms 236, 44–54.
Colin, X., Marais, C., Verdu, J., 2002. Kinetic modelling and simulation of gravimetric curves: application to the oxidation of bismaleimide and epoxy resins. Polym. Degrad. Stabil. 78, 545–553.
Datsyuk, V., Trotsenko, S., Trakakis, G., Boden, A., Vyzas-Asimakopoulos, K., Parthenios, J., Galiotis, C., Reich, S., Papagelis, K., 2020. Thermal properties enhancement of epoxy resins by incorporating polybenzimidazole nanofibers filled with graphene and carbon nanotubes as reinforcing material. Polym. Test. 82, 106317.
Farkas, J., 1998. Irradiation as a method for decontaminating food: a review. Int. J. Food Microbiol. 44, 189–204.
Flaifel, M.H., Ahmad, S.H., Hassan, A., Bahri, S., Tarawneh, M.a.A., Yu, L.-J., 2013. Thermal conductivity and dynamic mechanical analysis of NiZn ferrite nanoparticles filled thermoplastic natural rubber nanocomposite. Compos. B Eng. 52, 334–339.
Gabr, M.H., Okumura, W., Ueda, H., Kuriyama, W., Uzawa, K., Kimpara, I., 2015. Mechanical and thermal properties of carbon fiber/polypropylene composite filled with nano-clay. Compos. B Eng. 69, 94–100.
Genovese, L., Lotti, N., Gazzano, M., Siracusa, V., Dalla Rosa, M., Munari, A., 2016. Novel biodegradable aliphatic copolyesters based on poly (butylene succinate) containing thioether-linkages for sustainable food packaging applications. Polym. Degrad. Stabil. 132, 191–201.
Hida, S., Hori, T., Shiga, T., Elliott, J., Shiomi, J., 2013. Thermal resistance and phonon scattering at the interface between carbon nanotube and amorphous polyethylene. Int. J. Heat Mass Tran. 67, 1024–1029.
Ismail, N.H., Mustapha, M., 2018. A review of thermoplastic elastomeric nanocomposites for high voltage insulation applications. Polym. Eng. Sci. 58, E36–E63.
Khare, N., Limaye, P., Soni, N., Patel, R., 2015. Gamma irradiation effects on thermal, physical and tribological properties of PEEK under water lubricated conditions. Wear 342, 85–91.
Kumar, V., Gulati, K., Lal, S., Arora, S., 2020. Effect of gamma irradiation on tensile and thermal properties of poplar wood flour-linear low density polyethylene composites. Radiat. Phys. Chem. 108922.
Lafi, O.A., Imran, M.M., 2010. The effect of gamma irradiation on glass transition temperature and thermal stability of Se96Sn4 chalcogenide glass. Radiat. Phys. Chem. 79, 104–108.
Li, R., Gu, Y., Yang, Z., Li, M., Wang, S., Zhang, Z., 2015. Effect of γ irradiation on the properties of basalt fiber reinforced epoxy resin matrix composite. J. Nucl. Mater. 466, 100–107.
Liu, L., Grunlan, J.C., 2007. Clay assisted dispersion of carbon nanotubes in conductive epoxy nanocomposites. Adv. Funct. Mater. 17, 2343–2348.
Lu, H., Hu, Y., Xiao, J., Kong, Q., Chen, Z., Fan, W., 2005. The influence of irradiation on morphology evolution and flammability properties of maleated polyethylene/clay nanocomposite. Mater. Lett. 59, 648–651.
Makuuchi, K., Cheng, S., 2012. Radiation Processing of Polymer Materials and its Industrial Applications. John Wiley & Sons.
Mammadov, S., Khankishiyeva, R., Ramazanov, M., Akbarov, O., Akbarov, E., Akhundzada, H., 2017. Influence of gamma irradiation on structure and properties of nitrile-butadien rubber in presence of modified nano metals. Am. J. Polym. Sci. 7, 23–29.
Mehra, N., Mu, L., Ji, T., Yang, X., Kong, J., Gu, J., Zhu, J., 2018. Thermal transport in polymeric materials and across composite interfaces. Appl. Mater. Today 12, 92–130.
Menacher, M., Leisen, C., Drummer, D., 2017. Influence of radiation cross-linking on fiber orientation in vibration welds of Polyamide 66. Polym. Compos. 38, 489–495.
Miedzianowska, J., Masłowski, M., Strzelec, K., 2019. Thermoplastic elastomer biocomposites filled with cereal straw fibers obtained with different processing methods—preparation and properties. Polymers 11, 641.
Mohamed, A.A., Mahmoud, G.A., ElDin, M.E., Saad, E., 2020. Synthesis and properties of (Gum acacia/polyacryamide/SiO2) magnetic hydrogel nanocomposite prepared by gamma irradiation. Poly. -Plastics Technol. Mater. 59, 357–370.
Moustafa, A., Mounir, R., El Miligy, A., Mohamed, M.A., 2016. Effect of gamma irradiation on the properties of natural rubber/styrene butadiene rubber blends. Arab. J. Chem. 9, S124–S129.
Müller, K., Bugnicourt, E., Latorre, M., Jorda, M., Echegoyen Sanz, Y., Lagaron, J.M., Miesbauer, O., Bianchin, A., Hankin, S., Bölz, U., 2017. Review on the processing and properties of polymer nanocomposites and nanocoatings and their applications in the packaging, automotive and solar energy fields. Nanomaterials 7, 74.
Negrin, M., Macerata, E., Consolati, G., Quasso, F., Genovese, L., Soccio, M., Giola, M., Lotti, N., Munari, A., Mariani, M., 2018. Gamma radiation effects on random copolymers based on poly (butylene succinate) for packaging applications. Radiat. Phys. Chem. 142, 34–43.
Paula, M., Diego, I., Dionisio, R., Vinhas, G., Alves, S., 2019. Gamma irradiation effects on polycaprolactone/zinc oxide nanocomposite films. Polímeros 29.
Paydayesh, A., Pashaei Soorbaghi, F., Aref Azar, A., Jalali-Arani, A., 2019. Electrical conductivity of graphene filled PLA/PMMA blends: experimental investigation and modeling. Polym. Compos. 40, 704–715.
Perera, R., Albano, C., Gonzalez, J., Silva, P., Ichazo, M., 2004. The effect of gamma radiation on the properties of polypropylene blends with styrene–butadiene–styrene copolymers. Polym. Degrad. Stabil. 85, 741–750.
Rahman, M., Hoque, M.A., Rahman, G., Azmi, M., Gafur, M., Khan, R.A., Hossain, M.K., 2019. Fe2O3 nanoparticles dispersed unsaturated polyester resin based nanocomposites: effect of gamma radiation on mechanical properties. Radiat. Eff. Defect Solid 174, 480–493.
Razavi, S.M., Dadbin, S., Frounchi, M., 2014. Effect of gamma ray on poly (lactic acid)/poly (vinyl acetate-co-vinyl alcohol) blends as biodegradable food packaging films. Radiat. Phys. Chem. 96, 12–18.
Romanov, N., Zakharova, I., Malova, M., Elistratova, M., Musikhin, S., 2018. Effect of gamma radiation on the thin nanocomposite MEH-PPV/C60 films, St. Petersburg Polytechnical State University Journal. Phys. Math. 11, 22–32.
Rui, E., Yang, J., Li, X., Ma, G., 2015. Effect of proton irradiation on mechanical properties of low-density polyethylene/multiwalled carbon nanotubes composites. Polym. Compos. 36, 278–286.
Sanusi, O.M., Benelfellah, A., Hocine, N.A., 2020. Clays and carbon nanotubes as hybrid nanofillers in thermoplastic-based nanocomposites–A review. Appl. Clay Sci. 185, 105408.
Song, S.H., 2018. The effect of clay/multiwall carbon nanotube hybrid fillers on the properties of elastomer nanocomposites. Int. J. Polym. Sci. 2018, 5295973.
Tarawneh, M.a.A., Ahmad, S.H., EhNoum, S., Lau, K.-t., 2013. Sonication effect on the mechanical properties of MWCNTs reinforced natural rubber. J. Compos. Mater. 47, 579–585.
Tarawneh, M.a.A., Chen, R.S., Hj Ahmad, S., Al-Tarawni, M.A.M., Saraireh, S.A., 2019. Hybridization of a thermoplastic natural rubber composite with multi-walled carbon nanotubes/silicon carbide nanoparticles and the effects on morphological, thermal, and mechanical properties. Polym. Compos. 40, E695–E703.
Tarawneh, M.a.A., Saraireh, S.A., Chen, R.S., Ahmad, S.H., Al-Tarawni, M.A.M., Al-Tweissi, M., Yu, L.J., 2020. Mechanical, thermal, and conductivity performances of

novel thermoplastic natural rubber/graphene nanoplates/polyaniline composites. J. Appl. Polym. Sci. 137, 48873.
Thakur, A.K., Kumar, P., Srinivas, J., 2016. Studies on effective elastic properties of CNT/Nano-Clay reinforced polymer hybrid composite. IOP Conference Series: Materials Science and Engineering. IOP Publishing, 012007.
Tüzemen, M.Ç., Salamcı, E., Avcı, A., 2017. Enhancing mechanical properties of bolted carbon/epoxy nanocomposites with carbon nanotube, nanoclay, and hybrid loading. Compos. B Eng. 128, 146–154.
Youssef, H.A., Abdel-Monem, Y.K., Diab, W.W., 2017. Effect of gamma irradiation on the properties of natural rubber latex and styrene-butadiene rubber latex nanocomposites. Polym. Compos. 38, E189–E198.
Yu, L.-J., Ahmad, S.H., Tarawneh, M.A., Razak, S.B.B.A., Natarajan, E., Ang, C.K., 2019. Magnetic, thermal stability and dynamic mechanical properties of beta isotactic polypropylene/natural rubber blends reinforced by NiZn ferrite nanoparticles. Defence Technol. 15, 958–963.
Zaidi, L., Bruzaud, S., Kaci, M., Bourmaud, A., Gautier, N., Grohens, Y., 2013. The effects of gamma irradiation on the morphology and properties of polylactide/Cloisite 30B nanocomposites. Polym. Degrad. Stabil. 98, 348–355.
Zailan, F.D., Chen, R.S., Shahdan, D., Ahmad, S., 2019. Effect of conductive polyaniline in thermoplastic natural rubber blends on the mechanical, thermal stability, and electrical conductivity properties. J. Appl. Polym. Sci. 136, 47527.
Zdiri, K., Elamri, A., Hamdaoui, M., Harzallah, O., Khenoussi, N., Brendlé, J., 2018. Reinforcement of recycled PP polymers by nanoparticles incorporation. Green Chem. Lett. Rev. 11, 296–311.